ISSN 2347 - 3983
Volume 9. No. 9, September 2021
International Journal of Emerging Trends in Engineering Research
Available Online at http://www.warse.org/IJETER/static/pdf/file/ijeter07992021.pdf
https://doi.org/10.30534/ijeter/2021/07992021

Effect of Upstream Ramp on Film-Cooling effectiveness

Abdelkader Lahcene[1], Nabil Benamara[2], Mohamed Benguediab[3]
[1] Laboratory of Materials and Reactive Systems -University DjillaliLiabes of SidiBel Abbes, Algeria, lhkader@yahoo.fr
[2]Laboratory of Materials and Reactive Systems -University DjillaliLiabes of SidiBel Abbes, Algeria, Benamaara96@yahoo.fr
[3]Laboratory of Materials and Reactive Systems -University DjillaliLiabes of SidiBel Abbes, Algeria, benguediabm@gmail.com

Received Date : August 03, 2021 Accepted Date : August 23, 2021 Published Date : September 07, 2021

ABSTRACT

Several techniques have been studied to improve the effectiveness of film cooling. One of these techniques involves the use of small obstacles to the removal holes injection. Objective of this study is to determine numerically the effect of the geometry and the obstacle position lover injection holes inclined 35 °, for the case of a flat plate provided with multi perforated. The results showed that the cooling efficiency can be improved by over 40% compared to a simple cooling by film cooling; the best optimal values were derived have regarding the distance between the obstacle and the holes injection.

Key words: Film cooling, Effectiveness, obstacle, holes, injection, model, adiabatic film, Fluent.

1. INTRODUCTION

To improve power and thermal efficiency, the increase in the operating temperature of the turbines is essential and can reach temperatures above 1200°C [1,2]. But these hightemperatures can shorten the life of the turbine and affect thermal efficiency [3].To circumvent the limit imposed by the allowable temperature of the blade metal, it is important to employ an advanced cooling method such as film cooling. Film cooling is an advanced technique used primarily for cooling gas turbine blades. This technique consists of injecting a secondary flow with a relatively low temperature on the external surface of the organ to protect from the thermal effects of the combustion gases. The behavior of an isolated jet, confined to a transverse flow (Figure 1) has been extended both experimentally and numerically. It follows from these studies that, depending on the rate of injection of the jet, a separation of the boundary layer and a zone of very high level of turbulence are produced immediately downstream of the point of injection. The jet behaves like a flexible solid body with a strongly three-dimensional structure. Upstream of the jet, the flow is braked as if it were falling against a solid wall (impact) causing an area of low pressure just downstream. This depression is directly responsible for the curvature of the jet in the direction of the main flow.

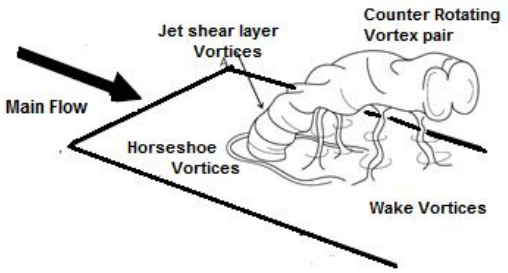

Figure 1: Perpendicular jet to the wall in longitudinal main flow.

The flow around the jet is characterized by a set of vortices of varying intensity and size. Under the effect of the two counter-rotating longitudinal vortices, the cross section of the jet takes on a shape reminiscent of a kidney. These two vortices have the detrimental effect of returning the hot fluid from the main flow to the flat wall, which defeats the desired corn. Due to the complex flow and heat transfer phenomena that accompany this type of cooling, several studies have been carried out on the effects of different parameters on the film cooling process [4,5]. From a thermal and aerodynamic point of view, the flow and heat transfer phenomena that accompany this cooling are very complex and require efforts to understand and control the various parameters acting on cooling.These parameters are classified into two categories: geometric parameters and thermo-hydrodynamic parameters. Studies on the effects of the geometry, inclination and orientation of injection holes have been by Ahn et al. [6], Goldstein [7], Rhee et al [8] and the blow-off rate on cooling efficiency [9, 10]. Despite the difficulty to use this process in a real situation and the complex flow and heat transfer phenomena in discrete-hole film cooling, theoretical, experimental and numerical studies have been carried out [11,13]. In these studies several geometric parameters such as the pitch of the positioning of the holes, the flared holes, the injection angle and the geometry of the plenum were studied. Khadem et al. [14] placed square obstacles upstream of the injection ports and measured the velocity fields, this study can

be considered one of the first experimental studies carried out on this type of cooling. The influence of the geometry of the injection holes in the presence of obstacles on the cooling efficiency has been investigated experimentally by Barigozzi et al [15]. Chen [16] have experimentally investigated the effect of the geometry and location of obstacles opposite to injection holes on the cooling of a plate. For a triangular geometry, he found that the presence of an obstacle only improves cooling performance at blowing rates greater than unity. Much research has oriented to control vortices to improve the cooling process per film, either by modifying the geometry of the hole itself, for example by using the compound [17] and / or profiled holes [18] or add fins placed at the level of the film cooling hole exit [19], using a converging slot hole [20, 21], or create a trench around a row of film cooling holes [22, 24]. In a recent study, Dinc et al. [25] have implemented a process for cooling the intake air has been implemented inthe admission of a land-based gas turbine engine for electricity. This process improves the performance of the turbine.

In this paper a numerical study of new configurations of obstacles and the effect of the size and position of the obstacle on the cooling efficiency for different values of blowing rates has been made.

2. GEOMETRICAL CONFIGURATION

The configuration studied is a flat plate provided with an injection hole, the main dimensions of which are shown in figure 2. The width of the slot (d) is 4 mm, the injection angle is 35 °, the width of the slot (d) is 4 mm, the injection angle is 35 °, length of the film slit is 10d, the computational domain has a length of 49 d and a height of 15 d.

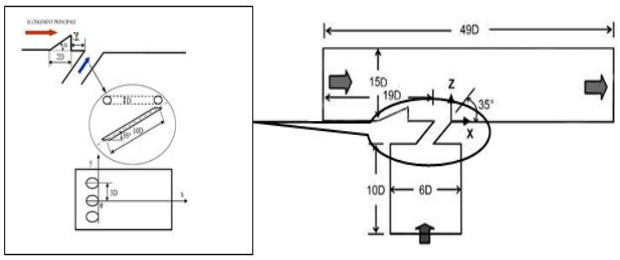

Figure 2: Geometry Configuration studied

Four typical blowing ratios M = 0.29; M = 0.57; M = 1.36 and M = 2 were studied. Flow parameters are set to correspond with the experiment, mainstream temperature Tg = 298 K and a free stream velocity Ug = 20 m/s in the X direction, jet temperature Tc = 188 K and the average velocity of the film-cooling holes Uc = 6 m/s. Perfect gas equation is applied in the calculation of the flow densities with pressure of 101 and 325 Pa and their temperatures. The mass-flux inlet boundary condition is set at the entry of the cooling hole and the value of mass flux is computed based on the values of U_g, M, ρ_g and ρ_c. Inlet turbulent intensities of the mainstream and the jet are 0.5% and 2%, respectively. The thermal boundary condition on the tested wall is adiabatic and its temperature is therefore the adiabatic wall temperature T_{aw}.

To examine the effect of the geometry and position of an obstacle on the cooling efficiency, we tested two types of obstacles round and triangular geometries for two positions 0.5D and D. In the case of a triangular obstacle, we consider three values of the inclination angle α= 8.5 °, 15 °, 24 °.

3. GOUVERNING EQUATIONS

The governing equations are three-dimensional Navier-Stokes equations. The basic set of equations solver by the program comprise equations for conservation of mass, momentum, and energy.

The continuity equation:

$$\frac{\partial \rho}{\partial t} + \nabla.(\rho\vec{U}) = 0 \qquad (1)$$

The momentum equation:

$$\frac{\partial \rho\vec{U}}{\partial t} + \nabla.\left((\rho\vec{U})\otimes\vec{U}\right) = \nabla p + \nabla\bar{\bar{\tau}} + \rho\vec{f} \qquad (2)$$

Energy equation:

$$\frac{\partial(\rho e)}{\partial t} + \vec{\nabla}.\left[(\rho e + p)\vec{U}\right] = \vec{\nabla}.\left(\bar{\bar{\tau}}.\vec{U}\right) + \rho\vec{f}.\vec{U} + \vec{\nabla}.(\dot{q}) \qquad (3)$$

Were ρ is the fluid density,$\vec{U} = (U, V, W)$ the fluid velocity, p the pressure, t is time.

$\bar{\bar{\tau}}$ is the component of the total stress tensor, $\vec{f}$ represents body forces (per unit volume) acting on the fluide total energy per unit mass, $\dot{q}$ is the heat flux.

3.1Thermal study of film cooling

The heat flux from flow to surface without film cooling is expressed as

$$q_0 = h_0(T_\infty - T_w) \qquad (4)$$

Where $h_0$the heat transfer coefficient without secondary jet, and $T_w$is the temperature local area of the wall, and T_∞ is mainstream temperature of the fluid in the undisturbed external zone (bulk).

In the presence of the cooling film, the local density of the heat flow can be described by expression (5):

$$q_0 = h_f(T_f - T_w) \qquad (5)$$

h_f : is the heat transfer coefficient with film cooling injection and T_f is local temperature of the film (mixture of mainstream and coolant). The determination of the temperature of the films is difficult .So a non-dimensional temperature is defined as

$$\eta = \frac{T_\infty - T_f}{T_\infty - T_c} \qquad (6)$$

$T_c$is the temperature of coolant, since de magnitude of T_f varies from T_c to $T_\infty T_c \le T_f \le T_\infty$ the value of η falls between from 0 to 1.

For an adiabatic wall the wall temperature in the absence of the film-cooling is $T_{aw} = T_{\infty}$

T_{aw}, is adiabatic wall temperature. So in the presence of the film cooling $T_{aw} = T_f$, a non-dimensional temperature is defined called adiabatic effectiveness

$$\eta = \frac{T_{\infty} - T_{aw}}{T_{\infty} - T_c} (7)$$

When $\eta = 0$, the surface is not under any film protection, this implies that the temperature of the adiabatic wall is equal to the temperature of the hot gas. On the other hand, $\eta = 1$ means that the temperature of the adiabatic wall is the temperature of the coolant, which indicates complete protection of the film.

In practical application we are interested to the laterally averaged adiabatic effectiveness defined by:

$$\overline{\eta} = \frac{1}{L_c} \int_0^L \eta(z) dz \quad (8)$$

Where L is the width of the surface to be cooled.

3.2 Turbulence Model

The turbulence model used is the RNG k-ε model with the standard wall law. In this turbulence model the Reynolds stresses and heat transfer are obtained by approximating eddy-viscosity and eddy-diffusivity respectively:

$$-\rho \overline{u'_i u'_j} = \mu_t \left(\frac{\partial U_i}{\partial x_j} + \frac{\partial U_j}{\partial x_i} \right) - \frac{2}{3} \mu_t \frac{\partial U_l}{\partial x_l} \delta_{ij} - \frac{2}{3} K \delta_{ij} \quad (9)$$

$$\rho \overline{u_i \theta} = -\frac{\mu_t}{\sigma \theta} \frac{\partial \theta}{\partial x_i} \quad (10)$$

Where

$$\mu_t = \rho C_{\mu} \frac{K^2}{\varepsilon}$$

The turbulent kinetic energy transport equations K and its dissipation rate ε are obtained from the resolution of the following equations:

$$\frac{\partial}{\partial t}(\rho \varepsilon) + \frac{\partial}{\partial x_i}(\rho U_i \varepsilon) = \frac{\partial}{\partial x_i}\left(\alpha \mu_{eff} \frac{\partial \varepsilon}{\partial x_i} \right) + C_{\varepsilon 1} \frac{\varepsilon}{K} \mu_i \left(\frac{\partial U_i}{\partial x_j} + \frac{\partial U_j}{\partial x_i} \right) \frac{\partial U_j}{\partial x_j} - C_{\varepsilon 2} \rho \frac{\varepsilon^2}{K} - R (11)$$

$$\frac{\partial}{\partial t}(\rho K) + \frac{\partial}{\partial x_i}(\rho U_i K) = \frac{\partial}{\partial x_i}\left(\alpha \mu_{eff} \frac{\partial K}{\partial x_i} \right) + \mu_i \left(\frac{\partial U_i}{\partial x_j} + \frac{\partial U_j}{\partial x_i} \right) \frac{\partial U_j}{\partial x_j} - \rho \varepsilon (12)$$

The empirical constants for the RNG K-ε model are:
C_{μ}= 0.0845; $C_{\varepsilon 1}$ = 1.42 and $C_{\varepsilon 2}$ = 1.68.

The system of equations associated with the boundary conditions is solved numerically by the finite volume method. The SIMPLE algorithm proposed by Patankar [26] is used for pressure and velocity correction. The hybrid scheme is used for the discretization of the convective terms in all the transport equations. Two types of mesh are used: triangular in the plenum and tetrahedral above his wall (figure 3). The calculations are performed using the FLUENT code.

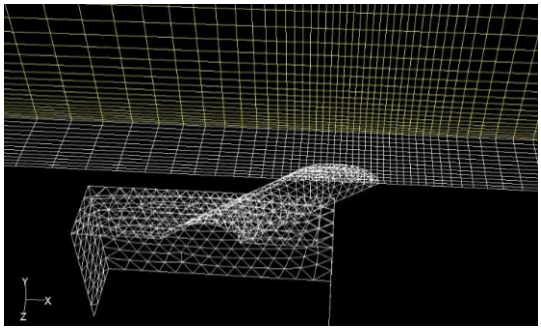

Figure 3: Types of Mesh

3.3 Grid Verification

To validate the choice of the mesh and numerical method used in this study calculation, the solution obtained for the problem of film cooling over a flat plate were compared with the experimental data provided by Chen [16] for L/D=2.8 at a blowing M=0.57 ratio of 0.5 . From the Fig.2, it can be seen that the centerline adiabatic effectiveness is over predicted. This indicates that the realizable k-ε model over predicts normal spreading of the cooling jet. Though the predictions may not be sufficiently accurate quantitatively, they may be good enough to provide insight on the flow and to discern differences in film-cooling designs.

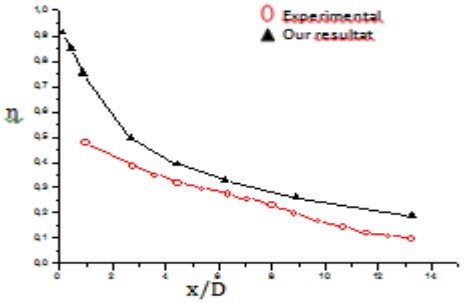

Figure 4: Comparison between numerical and experimental results[6] M=0.57; γ=D and α=24°

The quality of the grid plays an important role on the precision of the solutions and contributes greatly to minimizing the errors induced by the grid and to solving the relevant flux physics. A sensitivity study was made to find the appropriate grid. The results of this study in the case without a ramp, involving three grids: the basic grid with 2.291 million cells, a finer grid with 2.716 million cells (adaptation 1), and an even finer grid with 5.252 million cells (adaptation 2). For the two thinner grids, the extra cells were all concentrated around the film cooling hole and the hot gas / coolant-jet interaction region, where the physics of the flow are most complicated. From this grid sensitivity study, the baseline grid was found to give essentially the same result for midline adiabatic efficiency as that of matching grids 1 and 2.

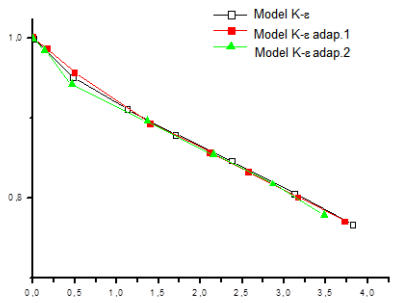

Figure 5: Grid-interdependence study: Centerline adiabatic effectiveness for three grids at M=0.57

The comparison between the results of the reference grid with those of the adaptation grid 2 gives a relative error in the adiabatic efficiency of the "average" median line is 0.4%. in figure 6 are represented the grids with and without upstream ramp used for this problem. Without the upstream ramp, the grid used comprises 2.291 million cells, on the other hand with an upstream ramp, the number of cells contained in the grid used varies from 2.282 million to 2.367 million, depending on the geometry and the angle ramp and its distance from the film cooling hole.

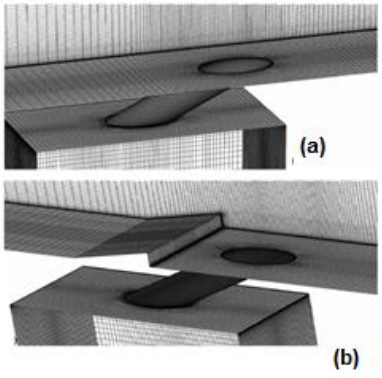

Figure 6: Grid used (a) without ramp (b) with ramp

4. RESULTS AND DISCUSSIONS

The results of the adiabatic efficiency of the film cooling are shown in Figure 7. These results show that with an upstream ramp, the adiabatic surface efficiency is greatly improved and that a much larger area around the film cooling hole is protected by the cooling jet, including the region upstream of the film-cooling hole. These results are logical with the nature of the fluid flow (Figure 8), the coolant is drawn downstream of the reverse of the rail by the recirculation flow in the separated region and the coolant spreads out laterally at the exit of the film cooling hole.

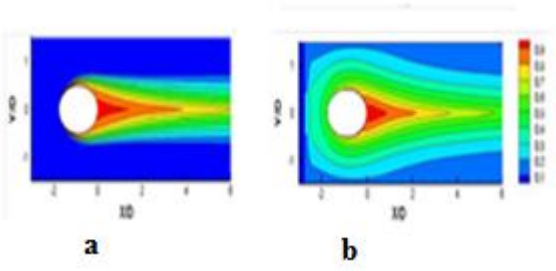

Figure 7: Adiabatic effectiveness for M=0.57 , γ = D and α = 24° (a) without ramp (b) with ramp

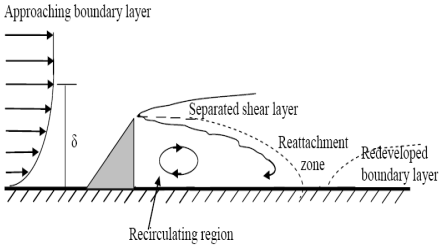

Figure 8: Schematic of the characteristics of flow over an upstream ramp [5]

The effects of the angle of the ramp and the distance between the pitch of the ramp oriented towards the rear and the cooling hole of the film are shown in Figures 9 and 10. We note for the two values of the angle studied, the adiabatic efficiency averaged laterally is high when the angle of the ramp (and therefore the height of the reverse gear) increases. Placing the ramp 0.5D upstream gives a higher mean adiabatic efficiency than a ramp placed 1.0D upstream.

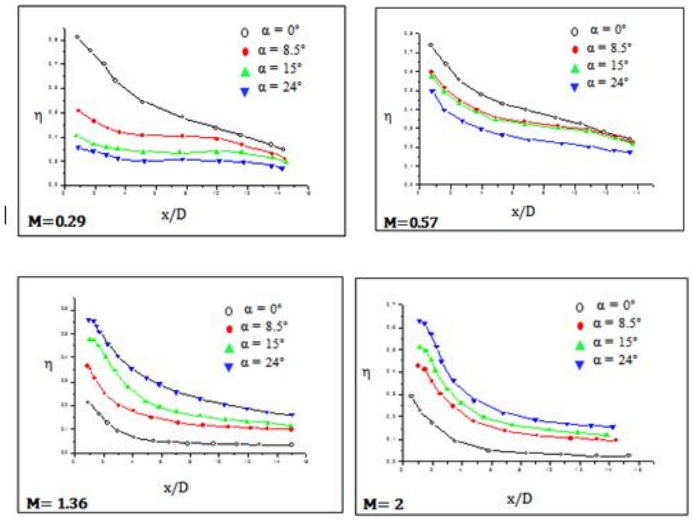

Figure 9 : Centerline film cooling effectiveness for different ramp angles at various blowing ratios

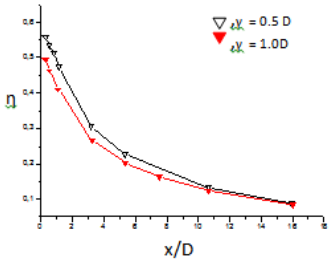

Figure 10 : Centerline film cooling effectiveness for different distance between ramp and film-cooling hole for M = 1.36 and α = 24°

Figure 11 contrasts the pressure coefficient on the film-cooled plate with and without an upstream ramp for the case with the most protruded ramp, which has a backward-facing step height of 1.0*D*.It can be seen that the ramp increases the pressure upstream of the backward-facing step and decreases the pressure downstream of it when compared to the case without the ramp. Thus, having a ramp increases pressure drag. The geometry of the ramp must be optimized to avoid the problem of pressure drag.

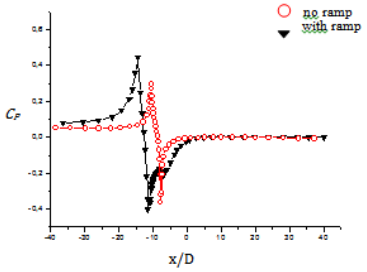

Figure 10 : Pressure coefficient on the plate along center line

4. CONCLUSION

The improvement in the adiabatic efficiency of film cooling is achieved by changing the geometry upstream of the film cooling holes. The effects of placing a ramp upstream of a row of film cooling holes were studied; the results obtained showed that a deviation of the boundary layer flux due to the ramp is obtained by approaching the base of the film cooling jet. An interaction between the boundary layer flow and the cooling jet farther from the surface is caused, eliminating the horseshoe vortex at the base of the cooling jet and allowing a wider lateral extent of the cooling jet of the movie. The coolant from the cooling film jet will spread from the region separated between the back step of the ramp and the cooling jet and to the cooling jet entraining a cooler fluid.

The ramps almost allow doubling the laterally averaged adiabatic effectiveness. However, it is necessary to optimize the geometry of the ramps, in order to avoid the problem of pressure formation in the cooling zone. This choice of geometry also depends on the blowing ratio.

REFERENCES

1. D. Straub, T. Sidwell, K. Casleton, S. Chien.**High temperature film cooling test facility and preliminary test,***ASME Turbo Expo, CopenhagenDenmark*, pp. 1661-1671, 2012.
2. M.K. Chyu, S.C. Siw.**Recent advances of internal cooling techniques for gas turbine airfoils,***Journal of Thermal Science and Engineering Applications* Vol.5,.2, 2013. https://doi.org/10.1115/1.4023829
3. Y. Çengel, M. Boles .**Thermodynamics: An engineering approach,***8th edition, McGraw-Hill Education*, New York 2015.
4. T. Fric, A., Roshko. **Vortical structure in the wake of a transverse jet,** *Journal of Fluid Mechanics*, Vol. 279,pp. 1-47. 1994. doi.org/10.1017/S0022112094003800.
5. K., Komuro, T, .Tsukiji.**Study On Vortical Structure of A Transverse Jet Using CfdFlucome**,*in Proc. 10 th International Conference on Fluid Control , Measurements and Visualization* , Moscow , pp. 1-9, 2009.
6. S. J. Ahn, I. S. Jung, J. S. Lee. **Film Cooling from Two Rows of Holes with Opposite Orientation Angles: Heat Transfer,***JSME International Journal*, Series B, Vol.43, p.706-711,2000.
7. R. J. Goldstein, P. Jin.**Film Cooling Downstream of a Row of Discrete Holes with Compound Angles**, *Journal of Turbomachinery*, Vol. 123, pp. 222-230,2001. https://doi.org/10.1115/1.1344905
8. H. H. Cho, D. H. Rhee, B.G. Kim.**Enhancement of Film Cooling Performance Using a Shaped Film Cooling Hole with Compound Angle Injection**, *JSME International Journal, Series B*, Vol. 44, n. 1, pp. 99-110, 2001. https://doi.org/10.1299/jsmeb.44.99
9. M.K. Kelishami, E. Lakzian. **Optimization of the blowing ratio for film cooling on a flat plate**, *International Journal of Numerical Methods for Heat & Fluid Flow*, Vol. 27, n.1, pp.104–119, 2017. https://doi.org/10.1108/HFF-07-2015-0284
10. M. Al-Hemyari, M.O. Hamdan, M.F. Orhan. **Numerical analysis of film cooling shield formed by confined jet discharging on a flat plate**,*International Journal of Heat and Technology*, Vol. 37, n. 1, pp. 327-333, 2019.
11. B.A. Haven, D.K. Yamagata, M. Kurosaka, S. Yamawaki, T. Maya.**Anti-Kidney Pair of Vortices in Shaped Holes and Their Influence on Film Cooling Effectiveness**, *In Proc. of the ASME International Gas Turbine and Aeroengine Congress and Exhibition. Volume 3: Heat Transfer; Electric Power; Industrial and Cogeneration*. Orlando, Florida, USA. 1997.
12. G. Wilfert, S. Wolff. **Influence of Internal Flow on Film Cooling Effectiveness,***ASME. J Turbomach.* Vol. 122, n.2, pp. 327–333, 2000.
13. C. Dang and H. Eiji.**Prediction of Cooling Heat Transfer Coefficient of Supercritical CO2 With Small Amount of Entraned Lubricating Oil Entrained by Neural Network Method,***International Refrigeration and Air Conditioning Conference**, Paper 908, Purdue e-Pubs 2008.

14. A.H. Khadem, L.J.S. Bradbury.**The distortion of a jet by tabs,***Journal of Fluid Mechanic*, vol. 70, pp. 801-813, 1975.
15. G. Barigozzi, G. Franchini, A. Perdichizzi.**The Effect of an Upstream Ramp on Cylindrical and Fan-shaped Hole Film Cooling,***Part I: Aerodynamic Results", GT2007-27077, ASME: Turbo Expo 2007:* Power for Land, Sea, and Air, Vol 4, Montreal, Canada, 105-113, doi:10.1115/GT2007-27077
16. S. Chen.**Film Cooling enhancement with surface restructure,** PhD. Dissertation, Pittsburgh University, 2007.
17. P. M. Ligrani, J. S. Lee.**Film cooling from two staggered rows of compound angle holes at high blowing ratios**, *Int. J. Rotating Mach.*, vol. **2**, n. 3, pp. 201–208, 1996.
18. R. S. Bunker. **A Review of Shaped Hole Turbine Film-Cooling Technology**, *ASME J. Heat Transfer*, Vol. 127, n.4; pp.441–453, 2005.
19. S. V.Ekkad, H. Nasir, S. Acharya. **Flat surface film cooling from cylindrical holes with discrete tabs,***J. Thermophys. Heat Transfer*, vol. 17, n. 3, pp. 304–312, 2003
20. J. E. Sargison, S. M. Guo, M. L. Oldfield, G. D. Lock, , A. J. Rawlinson. **A converging slot-hole film-cooling geometry, Part 1: Low-speed flat-plate heat transfer and loss,***ASME J. Turbomach.*, vol. 124, pp. 453–460, 2002.
21. J. E. Sargison, S. M. Guo, M. L. Oldfield, G. D. Lock, , A. J. Rawlinson.**A converging slot-hole film-cooling geometry, Part 2: Transonic nozzle guide vane heat transfer and loss,** *ASME J. Turbomach.*, vol. 124, pp. 461–471, 2002
22. A. Azzi, B.A. Jubran.**Numerical modelling of film cooling from converging slothole**, *Heat Mass Transfer* , Vol. 43:pp. 381–388,2007.
23. R. S. Bunker**. Film cooling effectiveness due to discrete holes within transverse surface slots**,*In Proc. of IGTI Turbo Expo,* Amsterdam, The Netherlands, ASME Paper no. GT 2002, 301178,2002.
24. S. Baheri, B. A. Jubran.**The effect of turbulence intensity on film cooling of gas turbine blade from trenched shaped holes,***J. Heat Mass Transfer*, vol. 48, n. 5, pp. 831–840, 2012
25. A. Dinc, I. Elbadawy, M.Fayed, R. Thaer, J.F. Derakhshandeh and Y. Gharbia.**Performance Improvement of a 43 MW Class Gas Turbine Engine with Inlet Air Cooling,***International Journal Emerging of Trends in Engineering Research,* Vol. 9, n°5,pp.539-544, 2021. https://doi.org/10.30534/ijeter/2021/01952021
26. S.V. Patankar, **Numerical Heat Transfer and Fluid Flow**,1st edition, CRC Press, 1980.